Rapid restoration of visual pigment and function with oral retinoid in a mouse model of childhood blindness

J. Preston Van Hooser*, Tomas S. Aleman†, Yu-Guang He*, Artur V. Cideciyan†, Vladimir Kuksa*, Steven J. Pittler‡, Edwin M. Stone§, Samuel G. Jacobson†, and Krzysztof Palczewski*¶‖**

Departments of *Ophthalmology, ¶Chemistry, and ‖Pharmacology, University of Washington, Seattle, WA 98195; †Scheie Eye Institute, Department of Ophthalmology, University of Pennsylvania, Philadelphia, PA 19104; ‡Vision Science Research Center, University of Alabama, Birmingham, AL 35294; and §University of Iowa Hospitals and Clinics, Department of Ophthalmology, Iowa City, IA 52242

Communicated by Hans Neurath, University of Washington, Seattle, WA, May 22, 2000 (received for review May 8, 2000)

Mutations in the retinal pigment epithelium gene encoding RPE65 are a cause of the incurable early-onset recessive human retinal degenerations known as Leber congenital amaurosis. *Rpe65*-deficient mice, a model of Leber congenital amaurosis, have no rod photopigment and severely impaired rod physiology. We analyzed retinoid flow in this model and then intervened by using oral 9-*cis*-retinal, attempting to bypass the biochemical block caused by the genetic abnormality. Within 48 h, there was formation of rod photopigment and dramatic improvement in rod physiology, thus demonstrating that mechanism-based pharmacological intervention has the potential to restore vision in otherwise incurable genetic retinal degenerations.

Two fundamental processes of vertebrate vision sustain light perception: transformation of the light signal into chemical changes within photoreceptor cells and a regeneration process involving the retinal pigment epithelial cells (RPE). Isomerization of the visual pigments' chromophore, 11-*cis*-retinal to all-*trans*-retinal, triggers a set of reactions collectively termed phototransduction (1, 2). The photolyzed product all-*trans*-retinal is reduced first in photoreceptors and then converted back to 11-*cis*-retinal in the RPE in an enzymatic process referred to as the visual cycle (3, 4). Molecular details are available on phototransduction events; however, the visual cycle is just attaining an understanding at the molecular level.

RPE65 is an RPE-specific protein (5, 6) postulated to play an important role in the visual cycle (7). Key to this hypothesis was the finding that *Rpe65*-deficient (*Rpe65*$-/-$) mice display a block in the visual cycle (7). The molecular defect in these mice leads to absence of 11-*cis*-retinal and rhodopsin, accumulation of all-*trans*-retinyl esters, severe impairment of rod photoreceptor function, and eventual retinal degeneration (7). In addition to the value of these experiments to increase knowledge of the molecular basis of vision, there is human clinical relevance. Mutations in the *RPE65* gene account for $\approx$10% of the childhood-onset retinal degenerations known as Leber congenital amaurosis (LCA) and some cases of recessive retinitis pigmentosa (8–10). Better understanding of mechanism in this murine model could lead to therapeutic strategies for these otherwise incurable human afflictions (11).

In this study, we took a first step toward intervention in LCA by targeting the visual cycle block in the *Rpe65*$-/-$ mouse with the goal of bypassing the biochemical defect. We probed mechanisms at a biochemical level, by characterizing the retinoid content and flow in the mouse model; and then, we performed 9-*cis*-retinal oral gavage experiments on the *Rpe65*$-/-$ mice. The results show that rod photopigment was formed and rod retinal function was rapidly restored in the *Rpe65*$-/-$ animals following oral treatment with the retinoid. Such experiments raise the hope that mechanism-based pharmacological interventions may be able to alter the blinding disease sequence of incurable genetic retinal degenerations.

Materials and Methods

***Rpe65* Mice and Retinoid Analyses.** Experiments were in accordance with institutional guidelines. Animals were maintained in complete darkness, and all manipulations were completed under dim red light. Progeny of matings were genotyped by *Rpe65*-specific 3-primer PCR (7, 12). Typically, 8- to 12-week-old mice were used in experiments. Retinoids were analyzed on a Hewlett Packard 1100 series HPLC, equipped with a diode-array detector and Hewlett Packard CHEMSTATION A.06.03 software, allowing full integration (13). The latter feature allowed the online recording of UV spectra and identification of retinoid isomers according to their specific absorption spectra. A normal phase, narrow-bore column (Alltech, silica 5u solvent miser, 2.1 $\times$ 250 mm) and an isocratic solvent composed of 4% ethyl acetate in hexane at a flow rate of 0.5 ml/min were used to separate retinoids. Rhodopsin measurements were performed as described recently (13). Typically, two mouse eyes were used per assay and repeated three to six times. The data are presented with SEM. In addition, all experimental procedures related to the analyses of dissected mouse eyes, derivatization, and separation of retinoids have been described in detail previously (14, 15)

Analysis of Oil Droplet-Like Structures. Eyes from *Rpe65*$+/+$ and *Rpe65*$-/-$ mice were enucleated and anterior segments removed. The posterior pole was incubated in water to release hydrophobic structures with densities lower than water. The sample was centrifuged at 30,000 $\times$ *g* for 15 min at 4°C. The top layers were harvested and extracted with hexane and analyzed by HPLC.

Preparation of Retinoids and Oral Gavage. Retinoids were prepared as follows: 9-*cis*-retinal (15 mg, 52.8 μmol, Sigma) was dissolved in absolute EtOH (1 ml), and solid $NaBH_4$ (6.0 mg, 159 μmol) was added. After 30 min at 0°C, water (2 ml) was added and 9-*cis*-retinol was extracted with hexane (4 $\times$ 1 ml). Hexane was evaporated under a stream of argon at 30°C, and 9-*cis*-retinol (10 mg) was used in gavage experiments without further purification. 9-*cis*-Retinol (20 mg, 70 μmol) was dissolved in dry CH_2Cl_2 (300 μl) and mixed with solutions of palmitoyl chloride (34.8 mg, 127 μmol) in CH_2Cl_2 (500 μl) and diisopropylethylamine (23 mg, 142 μmol) in CH_2Cl_2 (500 μl). The reaction mixture was kept at 0°C for 6 h. CH_2Cl_2 was evaporated under a stream of argon and the ester was purified on Whatman TLC plates by using 10:89:1% (vol) ethyl acetate:hexane:Et_3N.

9-*cis*-Retinal, 9-*cis*-retinol, and palmitoyl-9-*cis*-retinyl ester (0.25 ml), at a final concentration of 10 mg/ml in vegetable oil,

Abbreviations: LCA, Leber congenital amaurosis; ROS, rod outer segment; RPE, retinal pigment epithelial cells; ERG, electroretinogram; OCT, optical coherence tomography.

**To whom reprint requests should be addressed. E-mail: palczews@u.washington.edu.

The publication costs of this article were defrayed in part by page charge payment. This article must therefore be hereby marked "*advertisement*" in accordance with 18 U.S.C. §1734 solely to indicate this fact.

Article published online before print: *Proc. Natl. Acad. Sci. USA*, 10.1073/pnas.150236297. Article and publication date are at www.pnas.org/cgi/doi/10.1073/pnas.150236297

were administered to *Rpe65*−/− mice by using a 1-ml syringe and a 20-gauge, 3.5-cm long gavage needle.

Mouse Electroretinograms (ERGs). Mice were anesthetized with ketamine (65 mg/kg, i.p.) and xylazine (5 mg/kg, i.p.); corneal anesthesia was attained with topical proparacaine HCl (1%), and pupils were dilated with tropicamide (1%) and phenylephrine (2.5%). Full field ERGs were recorded from one eye of each animal by using a computer-based system (EPIC-XL, LKC Technologies, Gaithersburg, MD) and contact lens electrodes. Depending on stimulus strength, murine ERGs can have two major features, a cornea-negative a-wave and a cornea-positive b-wave. Dark-adapted luminance-response functions for b-waves were obtained with blue (Wratten 47A) flash stimuli (−3.8 to −0.3 log scot-cd·s·m^{-2}). B-wave amplitudes were measured conventionally from baseline or a-wave trough to positive peak. ERG photoresponses (a-waves with a saturated amplitude) were evoked under dark-adapted conditions with 2.2 and 3.6 log scot-cd·s·m^{-2} flashes. Leading edges of the two ERG photoresponses were fitted (as an ensemble) with a model of rod phototransduction activation (16). Leading edges of ERG photoresponses represent the sum of light induced dark-current shut-off in rod photoreceptor outer segments (17). Amplification constant for photoreceptors (18) can be calculated under appropriate assumptions. A ganzfeld stimulus of 1 scot-cd·s·m^{-2} presented to a pigmented mouse has been estimated to produce from ≈100 (19) to 1,500 (20) isomerizations per mouse rod.

Human Studies. A patient with LCA, her parents, her sibling, and normal control subjects were included. Informed consent was obtained from subjects after explanation of the procedures; all studies conformed to the Declaration of Helsinki. DNA was extracted from peripheral blood and screened for coding sequence mutations in the *RPE65* gene (21). The patient and family members underwent complete eye examinations, Goldmann kinetic perimetry, and optical coherence tomography (OCT). Selected members had ERGs and static threshold perimetry (22). For static threshold perimetry in the patient, dark-adapted and light-adapted (2.7 log troland) testing used white stimuli (22). Details of the ERG, psychophysical and OCT methods, and normal data have been published (22, 23).

Results and Discussion

Analysis of Retinoid Flow in *Rpe65* Mice. Baseline studies of retinoids and rhodopsin in the eyes of *Rpe65*+/+, *Rpe65*+/−, and *Rpe65*−/− mice were performed by using HPLC and UV/visible spectroscopy (Fig. 1). In dark-adapted *Rpe65*+/+ mice, the major retinoid components were retinyl ester (250 ± 24 pmol/eye, >95% as all-*trans*-retinyl esters) and 11-*cis*-retinal (565 ± 34 pmol/eye) (Fig. 1*A*) (13, 24). Only small amounts (<40 pmol/eye) of all-*trans*-retinal and 11-*cis*-retinol were present. *Rpe65*+/− mice had retinoid components similar to those of *Rpe65*+/+ mice (Fig. 1*A*). Consistent with previous results (7), *Rpe65*−/− mice showed elevated levels of retinyl esters (1,250 ± 25 pmol/eye) and no detectable amounts of any other retinoids, including 11-*cis*-retinal. Osmotic shock treatment of *Rpe65*−/− mouse eyes revealed the presence of retinyl esters at ≈1,000-fold higher concentration as compared to *Rpe65*+/+. This suggested that the major retinoid component of droplet-like deposits seen in the RPE of *Rpe65*−/− mice (7) was all-*trans*-retinyl ester. There was no detectable rhodopsin in *Rpe65*−/− mice but rhodopsin in *Rpe65*+/− mice (578 ± 54 pmol/eye) was like that in *Rpe65*+/+ mice (542 ± 33 pmol/eye) (Fig. 1*B*). Our analysis confirms that the isomerization step is affected in *Rpe65*−/− mice (7).

We sought to clarify the role of RPE65 in the retinoid cycle by examining the kinetics of retinoid flux after significant bleach in *Rpe65*+/− mice. Such an analysis in *Rpe65*−/− mice is uninformative because of the lack of any retinoids other than all-*trans*-retinyl esters. After a flash that bleached ≈40% rhodopsin, all-*trans*-retinal was reduced with a $t_{1/2}$ of ≈15 min in *Rpe65*+/− mice (Fig. 1*Ca*). This rate was comparable to the rate obtained for *Rpe65*+/+ mice. No significant accumulation of all-*trans*-retinol was detected as compared to total amounts of retinoids (*b*). There was a delayed abnormal accumulation of all-*trans*-retinyl esters in *Rpe65*+/− mice that peaked at 30 min (*c*) and then declined at a rate of ≈2.6 pmol/min. No significant accumulation of 11-*cis*-retinol was found (*d*), suggesting that the oxidation to 11-*cis*-retinal is unaffected. The rate of 11-*cis*-retinal formation was 2.1 pmol/min (*e*), comparable to the rate of retinyl ester decrease and ≈5-times slower than the rate for *Rpe65*+/+ mice. In agreement with these results, the rate of rhodopsin regeneration in *Rpe65*+/− mice was 2.2 pmol/min and also ≈5-times slower than the regeneration rate for *Rpe65*+/+ mice (not shown). Using Western analysis and scanning spectrometry, we measured that *Rpe65*+/− mice contained ≈50% of RPE65 protein as compared to *Rpe65*+/+ mice (not shown). RPE65 could be thus a nonenzymatic protein, and a lack of RPE65 blocks the retinoid cycle at the level of the hydrolysis of retinyl ester or isomerization.

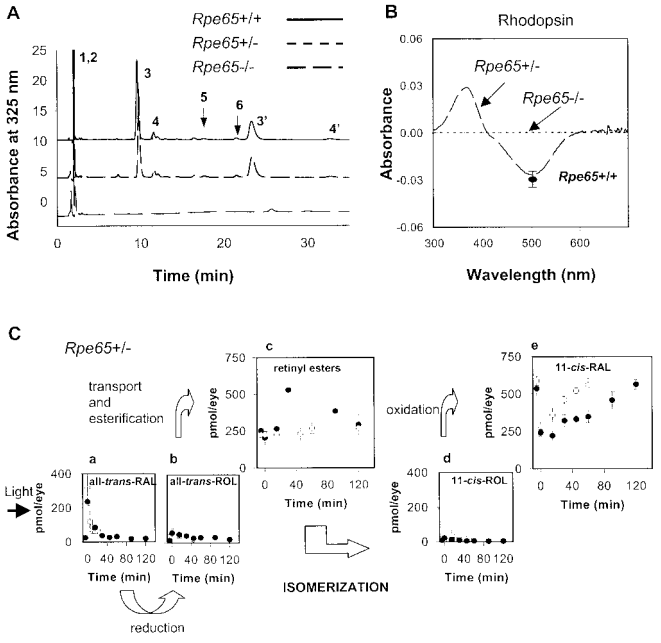

Fig. 1. Retinoid and rhodopsin analysis in *Rpe65* mice. (*A*) Chromatogram of retinoids extracted from eyes of *Rpe65*+/+, *Rpe65*+/−, and *Rpe65*−/− mice. The extraction procedures and derivatization with hydroxylamine to improve quantitative extraction of retinaldehydes were described previously (see ref. 13). Peaks are represented as follows: (1, 2) all-*trans*-retinyl and 11-*cis*-retinyl esters (truncated to fit in scale); (3,3′) *anti*- and *syn*- of 11-*cis*-retinal oximes; (4,4′) *anti*- and *syn*- of all-*trans*-retinal oximes; (5) 11-*cis*-retinol, and (6) all-*trans*-retinol. (*B*) Difference spectrum of bleached rhodopsin and rhodopsin extracted from eyes of *Rpe65*+/− and *Rpe65*−/− mice. The level of rhodopsin in *Rpe65*+/− mice is within the range of rhodopsin found in control *Rpe65*+/+ mice (●) and undetectable in *Rpe65*−/− mice. (*C*) Aberrant kinetics of retinoid and rhodopsin recovery in *Rpe65*+/− mice after a flash. Photolyzed rhodopsin releases all-*trans*-retinal (*a*), which is reduced to all-*trans*-retinol (*b*), and then transported to the RPE and esterified to retinyl esters (*c*). All-*trans*-retinol, or its derivative, is isomerized to 11-*cis*-retinol (*d*), which in turn, is oxidized to 11-*cis*-retinal (*e*). The rates of retinoid formations are compared to the rate obtained for *Rpe65*+/+ mice (○).

Bypassing the Visual Cycle Defect of *Rpe65*−/− Mice. To bypass this defect in the retinoid cycle, we introduced synthetic *cis*-retinoids by oral gavage in *Rpe65*−/− mice at an age (8–12 wk) when there were only minimal changes in photoreceptor morphology

(7). We chose commercially available 9-*cis*-retinal because it forms the visual pigment isorhodopsin (25), which when bleached, undergoes conformational changes through the same photoproducts as 11-*cis*-retinal regenerated rhodopsin, and is thermodynamically more stable than 11-*cis*-retinal. In addition, isorhodopsin has an absorption maximum hypsochromicly shifted by 8 nm (λ = 494 nm), as compared to rhodopsin (λ = 502 nm). This difference provided additional verification of the genetic status of tested mice. 9-*cis*-Retinal also is not detectable in the *Rpe65*+/+ retina; thus, if isorhodopsin is formed, it resulted from added retinoids and not from activation of the metabolic pathway that would lead to 11-*cis*-retinal production. If formation of isorhodopsin triggers production of 11-*cis*-retinal, both isomers could be concurrently detected. Furthermore, 9-*cis*-retinal injected i.p. into vitamin A-deprived rats has been shown to result in formation of isorhodopsin (26).

Administration of 9-*cis*-retinal (2.5 mg) led to production of isorhodopsin as confirmed by hypsochromic shift on UV/visible spectroscopy (Fig. 2*A*). The maximal effect was observed at ≈48 h after gavage (2.5 mg/animal). Lower doses (0.5 mg/animal) also led to the production of isorhodopsin, but at lower levels (Fig. 2*B*). 9-*cis*-Retinol and 9-*cis*-retinyl ester yielded ≈30% of the isorhodopsin formed by 9-*cis*-retinal gavage. We attributed this finding to the high instability of retinol and retinyl esters at gastric low pH (K.P., unpublished data). Mice administered all-*trans*-retinal did not show any detectable rhodopsin or free 11-*cis*-retinal. Under similar conditions, mice treated with 11-*cis*-retinal formed only ≈50% of rhodopsin compared to 9-*cis*-retinal-dependent formation of isorhodopsin. Transmission of 9-*cis*-retinal from mothers to their offspring during pregnancy or through nursing was demonstrable but limited. When an *Rpe65*−/− female (mated with an *Rpe65*−/− male) was administered 2.5 mg of 9-*cis*-retinal at approximately day 12 of pregnancy, 20 ± 9 pmol/eye isorhodopsin was formed in the offspring. Oral gavage of 9-*cis*-retinal to *Rpe65*+/+ and *Rpe65*+/− mice led to a trace level of 9-*cis*-isomers in the eye.

Formation of isorhodopsin in *Rpe65*−/− mice treated with 9-*cis*-retinal was confirmed by HPLC analysis of retinoids (Fig. 2*C*). Because of precolumn derivatization, 9-*cis*-retinal was isolated as a mixture of *syn*- and *anti*-9-*cis*-retinal oximes (peak 7,7′). Because the amounts of 9-*cis*-retinal oximes were similar to the amounts of isorhodopsin (<8% differences between samples), these results suggest that the aldehyde is present almost exclusively in the bound form to opsin. Bleaching produced all-*trans*-retinal (seen as oximes 4 and 4′). Next, the all-*trans*-retinal is reduced to all-*trans*-retinol and most likely esterified, whereas 9-*cis*-retinal recovered with time (Fig. 2*C*). In all samples, there were also high levels of free all-*trans*-retinol, likely because of high concentrations of all-*trans*-retinyl esters. This elevated level of all-*trans*-retinol was not observed in the eyes of *Rpe65*+/+ mice. The analysis of isomeric composition of isolated retinyl esters, after saponification and rechromatography, showed accumulation of 9-*cis*-retinol (≈150–250 pmol/eye) and the presence of dominant all-*trans*-retinol (Fig. 2*C*, *Inset*). Bleaching led to formation of all-*trans*-retinal, which was metabolized rapidly (<15 min), and to small amounts of 11-*cis*-retinal (Fig. 2*C*, peak 3). The rate of isorhodopsin recovery after a flash in *Rpe65*−/− mice was similar to recovery of rhodopsin in *Rpe65*+/+ animals (Fig. 2*D*) suggesting normal kinetics of this "artificial" retinoid cycle.

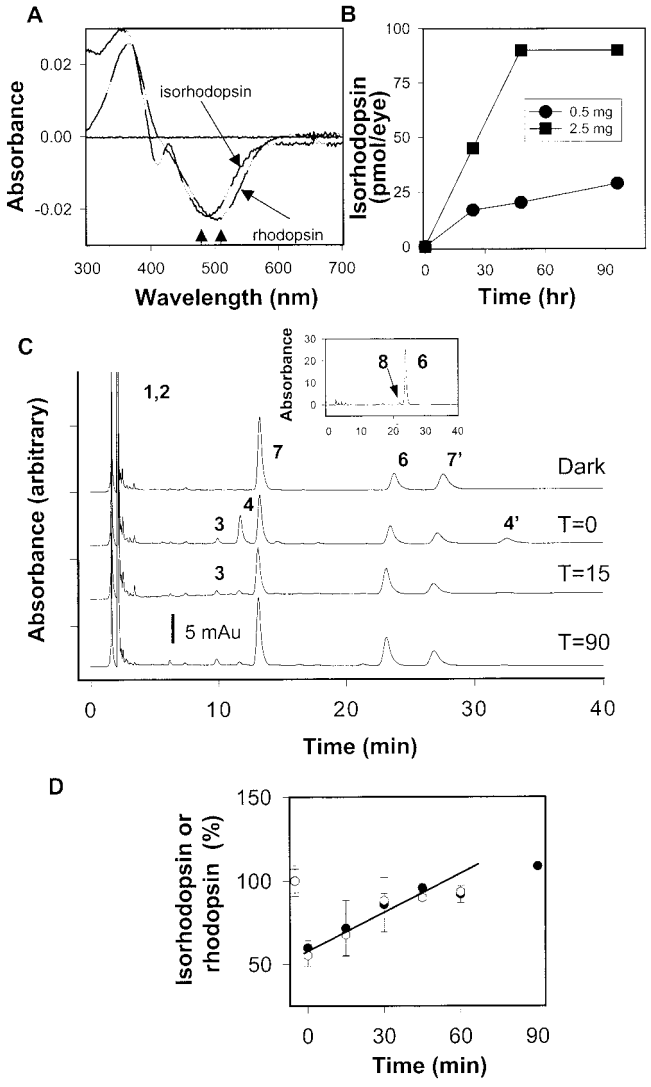

Fig. 2. Formation of isorhodopsin and kinetics of the retinoid flow in *Rpe65*−/− mice 48 h after 9-*cis*-retinal gavage. (*A*) Comparison spectra of rhodopsin from *Rpe65*+/+ mice and isorhodopsin from *Rpe65*−/− mice 48 h after 9-*cis*-retinal gavage (2.5 mg). Arrows denote differences in the absorption maximum for rhodopsin and isorhodopsin. (*B*) Isorhodopsin formation in *Rpe65*−/− mice at different time points after 0.5 mg or 2.5 mg of 9-*cis*-retinal gavage (n = 2). (*C*) Chromatograms illustrate the dark recovery of retinoids in *Rpe65*−/− mice 48 h after 9-*cis*-retinal gavage (2.5 mg) after a flash that bleached ≈45% of isorhodopsin. (*C*, *Inset*) isomeric composition of retinyl esters (8, 9-*cis*-retinol). (*D*) Dark recovery of isorhodopsin in *Rpe65*−/− mice 48 h after 9-*cis*-retinal gavage after a flash. For comparison, dark recovery of rhodopsin is shown for *Rpe65*+/+ (open hexagons) (7, 7′). *anti*- and *syn*- of 9-*cis*-Retinal oximes; all other peaks are as in the Fig. 1 legend.

Restored Retinal Physiology in *Rpe65*−/− Mice After 9-*cis*-Retinal. The impact of 9-*cis*-retinal administration on the visual physiology of *Rpe65*−/− mice was determined *in vivo* with ERG. Rod retinal function of untreated *Rpe65*−/− mice was detectable but impaired (Fig. 3). Dark-adapted ERGs were performed serially in an *Rpe65*−/− mouse before and 48 h after 9-*cis*-retinal gavage (Fig. 3 *A* and *B*). Before treatment, ERG b-wave threshold was elevated by ≈3 log units compared to *Rpe65*+/+; to the brighter stimuli, only a small b-wave was present and it resembled the normal response at threshold. The posttreatment recording had a lower b-wave threshold and increased amplitude. ERG photoresponses in this animal before treatment (Fig. 3*B*) had an abnormal maximum amplitude (R_{max} = 106 μV; normal mean ± SD = 335 ± 54 μV, n = 7) and sensitivity (S = 1.44 log scot-cd$^{-1}\cdot$ m$^2\cdot$s^{-3}; normal = 3.14 ± 0.13 log scot-cd$^{-1}\cdot$ m$^2\cdot$s^{-3}). The posttreatment parameters nearly doubled (R_{max} = 188 μV; S = 1.79 log scot-cd$^{-1}\cdot$m$^2\cdot$ s^{-3}) (Fig. 3*B*). Cross-sectional comparison of ERG photoresponse parameters in six other mice supported the

NEUROBIOLOGY

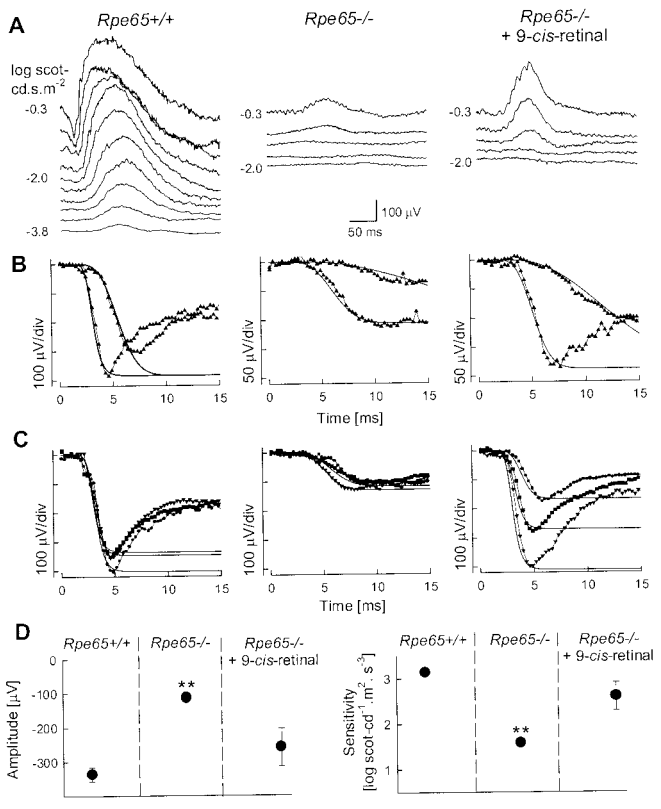

Fig. 3. Restoration of retinal function in *Rpe65*−/− mice 48 h after 9-*cis*-retinal gavage. (*A* and *B*) Serial ERG recordings in an *Rpe65*−/− mouse before and 48 h after 9-*cis*-retinal gavage compared to a representative *Rpe65*+/+ mouse. (*A*) Dark-adapted ERGs to increasing intensities of blue light stimuli (shown to the left of the traces) in an *Rpe65*−/− mouse show an elevated b-wave threshold compared to *Rpe65*+/+. The same stimuli after 9-*cis*-retinal treatment elicit ERGs at a lower threshold and with larger amplitude b-waves. (*B*) Leading edges (initial 4–15 ms depending on response) of dark-adapted ERG photoresponses (symbols) evoked by 3.6 and 2.2 log scot-cd·s·m^{-2} flashes are fit with a model of phototransduction (smooth lines). The amplitude and sensitivity of the *Rpe65*−/− mouse photoresponses are reduced. After 9-*cis*-retinal treatment, photoresponses have larger amplitude and higher sensitivity. (*C*) Photoresponses in three *Rpe65*+/+ mice are compared to an untreated group of *Rpe65*−/− mice and a treated group of *Rpe65*−/− mice. Lines are the model of rod phototransduction activation fitted to a pair of photoresponses; only maximal responses are shown for clarity. (*D*) Maximum amplitude and sensitivity parameters of dark-adapted photoresponses in untreated and treated (48 h after 9-*cis*-retinal gavage) *Rpe65*−/− mice compared to the results in *Rpe65*+/+ mice. Untreated animals have significant differences (**, $P < 0.05$) in both parameters when compared to *Rpe65*+/+ or treated *Rpe65*−/− mice. Error bars represent 1 SEM and are smaller than symbols for some data.

serial data in the one animal: three were untreated *Rpe65*−/− mice and three were *Rpe65*−/− mice 48 h after treatment with 9-*cis*-retinal (Fig. 3*C*). Posttreatment responses had greater R_{max} and S values (R_{max} =259 ± 111 μV; S = 2.60 ± 0.62 log scot-cd^{-1}·m^2·s^{-3}) than responses from the untreated mice (R_{max} =113 ± 13 μV; S = 1.58 ± 0.14 log scot-cd^{-1}·m^2·s^{-3}).

Statistically significant differences in ERG photoresponse parameters were found when *Rpe65*+/+, untreated *Rpe65*−/−, and treated *Rpe65*−/− groups were compared [(R_{max}, $F(2, 12) = 13.65$, $P = 0.0008$; S, $F(2, 12) = 28.68$, $P < 0.0001$); one-way ANOVA]. The group of untreated *Rpe65*−/− mice had significantly smaller mean R_{max} ($P < 0.05$; Tukey's studentized range test accounting for multiple comparisons) and mean S ($P < 0.05$) when compared to results of *Rpe65*+/+ and *Rpe65*−/− mice treated with 9-*cis*-retinal (Fig. 3*D*).

Role of RPE65 in the Visual Cycle. Our experimental results in *Rpe65*+/− and *Rpe65*−/− mice taken together with the postulated steps in the visual cycle provide significant insight into the potential role of RPE65. The observation that the recovery of rod pigment is ≈5-fold slower in *Rpe65*+/− mice as compared to *Rpe65*+/+ mice weighs against enzymatic properties of this protein; the anticipated reduction in the rate of a hypothetical enzymatic step in *Rpe65*+/− mice would be ≤2-fold. We cannot exclude the possibility that RPE65 may play a dual role: in addition to its putative enzymatic function, it also could be a structural protein. This protein is not involved in the reduction of all-*trans*-retinal, transport to RPE, and esterification, which are unaffected in *Rpe65*+/− mice. RPE65 also is not *cis*-retinyl specific retinyl hydrolase because 9-*cis*-retinyl ester is liberated promptly after bleach. RPE65 is not essential in the oxidation of the chromophore and transport back to ROS, considering that regeneration of isorhodopsin occurs even in the absence of RPE65. In newborn *Rpe65*−/− mice, all-*trans*-retinol trapped from the circulation deposits in RPE in the form of retinyl ester, but there is no rhodopsin formation, suggesting that retinyl esters are sequestered and not available for isomerization. Droplet-like structures analyzed after osmotic shock extraction also show major accumulation of retinyl ester in *Rpe65*−/− mice. The defect in *Rpe65*−/− mice is between retinyl ester and 11-*cis*-retinol production; however, three pieces of evidence weigh against RPE65 being the isomerase. First, dramatic reduction in rate of rod pigment recovery in *Rpe65*+/− mice suggest that this protein is not an enzyme. Second, there must be partial production of 11-*cis*-retinal as demonstrated physiologically by an insensitive but detectably functional rod system in *Rpe65*−/− mice. Third, there was a small amount of 11-*cis*-retinal formation detectable after a bleach in *Rpe65*−/− animals with orally administered 9-*cis*-retinal, suggesting that part of the all-*trans*-retinal released from bleached isorhodopsin may be available for 11-*cis*-retinal production without the RPE65 protein. Our results are in agreement with a recently reported biochemical observation that removal of RPE65 affected isomerization only to a small degree (27). RPE65 has been shown to interact with 11-*cis*-retinol dehydrogenase (28), and our data suggest that it could be involved in the intracellular distribution of retinyl esters in RPE. Specifically, RPE65 could be an organizer protein (an adapter) that secures the redistribution of retinyl esters, or a derivative, through the RPE for proper isomerization.

Human Relevance of These Murine Studies. An implicit assumption and the motivation for this work is that it may be clinically relevant. But what is the phenotype of the human disease it could benefit? There are many descriptions and subcategorizations of LCA from the premolecular era (for example refs. 29 and 30), but no detailed genotype-phenotype reports in the current literature to which the detailed studies in the murine model can be compared. We studied a homozygote with a putative null mutation in the *RPE65* gene with *in vivo* measurements of retinal function and "structure" (Fig. 4). The patient was shown to have a homozygous 20-bp deletion at codon 97 in *RPE65* (21, 31). From infancy onward, the patient had reduced vision, nystagmus, and a severely abnormal ERG. The parents and a male sibling were heterozygous for this deletion.

The homozygote, at age 11, had loss of peripheral visual field by kinetic perimetry (Fig. 4*A*). In the remaining field, dark-adapted thresholds were elevated by >6 log units, and there was >2 log units elevation under light-adapted conditions.

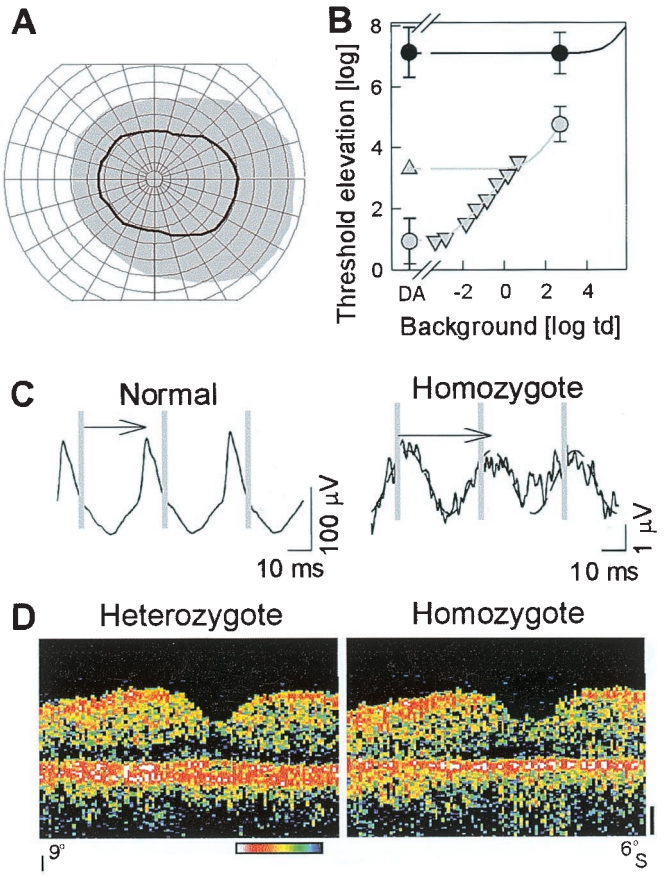

Fig. 4. Human phenotype of putative null mutation in *RPE65*. (*A*) Kinetic visual fields with a V-4e test target in the homozygote (black line) compared to normal (gray region); concentric circles are at 10° intervals and meridians are at 15°. (*B*) White stimulus thresholds of the homozygote (●) shows >6 log units of elevation under dark-adapted (DA) and >2 log units of elevation under light-adapted (2.7 log troland) conditions. Normal thresholds (gray symbols) on increasing background intensities (▽) and during the cone plateau following a full bleach (△) are fit with empirical models of background adaptation (gray lines) to define the rod- and cone-mediated limbs. The normal cone adaptation model was shifted by 3.8 log units to the right and up to fit the patient data (solid line). (*C*) Cone flicker ERGs in homozygote are reduced ≈100-fold in amplitude and abnormally delayed in timing (arrows). Vertical gray lines mark stimulus times. A 29-Hz sinusoid was fitted to the homozygote data (dashed lines) to estimate amplitude and timing of the small signal. (*D*) Vertical OCT cross-sectional retinal images through the fovea (9° inferior to 6° superior retina) show central retinal structure is generally intact in the homozygote (compared to a heterozygous sibling) except for thinning of the outer retina-choroid complex, the red/white band toward bottom of panel. Optical reflectivity of retinal tissue is shown on a logarithmic pseudocolor scale: red and white are high reflectivity and blue and black are low reflectivity. Vitreous is toward the top and sclera is toward the bottom.

Light adaptation did not change the visual sensitivity of the patient whereas it elevated normal thresholds by 4 log units (Fig. 4*B*). An empirical model of light adaptation fit to the patient data are consistent with >3.8 log units loss of cone sensitivity and >6.2 log units loss of rod sensitivity (32). Electrophysiology was consistent with psychophysics: there were no detectable rod ERGs and an abnormal cone flicker waveform with ≈100-fold reduced amplitude and delayed timing (Fig. 4*C*). Heterozygotes had normal clinical examinations, kinetic fields, dark- and light-adapted static perimetry, and ERGs.

Retinal structure in the context of this severe visual dysfunction in the homozygote was assessed by using cross-sectional retinal images acquired by OCT (Fig. 4*D*). The central retinal architecture of the homozygote, at age 11, was not grossly different from that of her age-similar heterozygous sibling (Fig. 4*D*), although some retinal degeneration is suggested by a thinning of the highly reflective (red) signal ascribed to the outer retina (photoreceptors-RPE-anterior choroid) (22, 23, 33). Although many other such genotype-phenotype studies are required for clarification, the results in this LCA patient suggest better preservation of structure than function, such as has been a feature of both murine and canine *RPE65*-associated retinopathies at early disease stages (7, 34, 35).

Further Questions Now Requiring Answers. A number of investigations have succeeded in slowing the rate of retinal degenerations (for example refs. 36–40), but dramatic reversal of retinal dysfunction in such disorders is a rarity (41–43). Our short-term experiments that reverse dysfunction in the *Rpe65*-deficient mouse prompt a multitude of questions. What effect, if any, does this intervention have on the natural history of the disease? Will it serve to retard the eventual retinal degeneration? The dosage and frequency of 9-*cis*-retinal administration need to be optimized. Will there be undue accumulation of all-*trans*-retinyl esters? 9-*cis*-Retinal may not be the ideal compound because of its light sensitivity. It appears to be the most efficient, among retinoids used in this study, in regenerating visual pigment. This isomer is more stable than 11-*cis*-retinal, and the aldehyde form is resistant to the acid conditions of the stomach. Most likely, 9-*cis*-retinal is reduced once absorbed in the epithelial cells and the toxicity is alleviated before the blood carries it. An encouraging observation made during the course of this study was that 11-*cis*-retinal was produced after 9-*cis*-retinal administration in *Rpe65*−/− mice. Under certain 9-*cis*-retinal treatment regimens, the endogenous production of 11-*cis*-retinal may be a valuable long lasting effect that could lead to prolonged recovery of vision.

It is critically important to understand the toxicity of retinoids and their clearance from the eye and liver (44). Analogs of 11-*cis*-retinal may be metabolized with different rates, and they themselves, and their degradation intermediates, could display different toxicity profiles. Other animal models need to be tested, like the *RPE65*−/− canine model (34, 35), to understand whether the effect of the retinoid treatment can be generalized. This study focused on rods, but to preserve cone vision, other compounds that lock rods in an inactive, light-insensitive state could be useful, assuming a cascade of degeneration leading from rod cell death to cone death (45, 46).

Could retinoid supplementation benefit patients with *RPE65*-associated LCA? Beyond the many safety and efficacy issues to be addressed experimentally, there is the immediate concern that severe retinal pathology in *RPE65*-LCA, specifically a major loss of photoreceptors, could nullify any potential benefit from this approach. ERG measurements of retinal function, helpful for diagnosis and monitoring, would not establish whether these patients are sensible candidates for intervention. *In vivo* estimates of retinal morphology, however, may be far more informative (22, 23, 33), especially when patients of known molecular subtype and similar dysfunction can be compared (47).

We especially thank Dr. T. Michael Redmond for providing *Rpe65* mice and help with the initial genotyping. We thank Dr. Françoise Haeseleer for help with initial genotyping of *Rpe65* mice and Dr. Maureen G. Maguire for statistical consultation. We gratefully acknowledge the excellent assistance of Daniel Marks, Beverly Miller, and Marcia Simovich. This research was supported by National Institutes of Health Grants EY09339 (to K.P.), EY05627 (to S.G.J.), and EY07031 (to Y.-G.H., Vision Training Grant), Research to Prevent Blindness, Inc., Foundation Fighting Blindness, Inc., Daniel Matzkin Research Fund, Stephen Wynn and Elaine Wynn Charitable Foundation, Ruth and Milton Steinbach Fund, and the E. K. Bishop Foundation.

1. Polans, A., Baehr, W. & Palczewski, K. (1996) *Trends Neurosci.* **19,** 547–554.
2. Lagnado, L. & Baylor, D. (1992) *Neuron* **8,** 995–1002.
3. Rando, R. R. (1996) *Chem. Biol.* **3,** 255–262.
4. Palczewski, K. & Saari, J. C. (1997) *Curr. Opin. Neurobiol.* **7,** 500–504.
5. Bavik, C. O., Busch, C. & Eriksson, U. (1992) *J. Biol. Chem.* **267,** 23035–23042.
6. Hamel, C. P., Tsilou, E., Pfeffer, B. A., Hooks, J. J., Detrick, B. & Redmond, T. M. (1993) *J. Biol. Chem.* **268,** 15751–15757.
7. Redmond, T. M., Yu, S., Lee, E., Bok, D., Hamasaki, D., Chen, N., Goletz, P., Ma, J. X., Crouch, R. K. & Pfeifer, K. (1998) *Nat. Genet.* **20,** 344–351.
8. Gu, S. M., Thompson, D. A., Srikumari, C. R. S., Lorenz, B., Finckh, U., Nicoletti, A., Murthy, K. R., Rathmann, M., Kumaramanickavel, G., Denton, M. J., *et al.* (1997) *Nat. Genet.* **17,** 194–197.
9. Marlhens, F., Bareil, C., Griffoin, J. M., Zrenner, E., Amalric, P., Eliaou, C., Liu, S. Y., Harris, E., Redmond, T. M., Arnaud, B., *et al.* (1997) *Nat. Genet.* **17,** 139–141.
10. Morimura, H., Fishman, G. A., Grover, S. A., Fulton, A. B., Berson, E. L. & Dryja, T. P. (1998) *Proc. Natl. Acad. Sci. USA* **95,** 3088–3093.
11. Rattner, A., Sun, H. & Nathans, J. (1999) *Annu. Rev. Genet.* **33,** 89–131.
12. Redmond, T. M. & Hamel, C. (2000) *Methods Enzymol.* **316,** 705–724.
13. Palczewski, K., Van Hooser, J. P., Garwin, G. G., Chen, J., Liou, G. I. & Saari, J. C. (1999) *Biochemistry* **38,** 12012–12019.
14. Garwin, G. G. & Saari, J. C. (2000) *Methods Enzymol.* **316,** 313–324.
15. Van Hooser, J. P., Garwin, G. G. & Saari, J. C. (2000) *Methods Enzymol.* **316,** 565–575.
16. Cideciyan, A. V. & Jacobson, S. G. (1996) *Vision Res.* **36,** 2609–2621.
17. Lyubarsky, A. L., Falsini, B., Pennesi, M. E., Valentini, P. & Pugh, E. N., Jr. (1999) *J. Neurosci.* **19,** 442–455.
18. Pugh, E. N., Jr. & Lamb, T. D. (1993) *Biochim. Biophys. Acta* **1141,** 111–149.
19. Hetling, J. R. & Pepperberg, D. R. (1999) *J. Physiol.* **516,** 593–609.
20. Pennesi, M. E., Lyubarsky, A. L. & Pugh, E. N., Jr. (1998) *Invest. Ophthalmol. Visual Sci.* **39,** 2148–2156.
21. Lotery, A. J., Namperumalsamy, P., Jacobson, S. G., Weleber, R. G., Fishman, G. A., Musarella, M. A., Hoyt, C. S., Heon, E., Levin, A., Jan, J., *et al.* (2000) *Arch. Ophthalmol.* **118,** 538–543.
22. Jacobson, S. G., Cideciyan, A. V., Huang, Y. J., Hanna, D. B., Freund, C. L., Affatigato, L. M., Carr, R. E., Zack, D. J., Stone, E. M. & McInnes, R. R. (1998) *Invest. Ophthalmol. Visual Sci.* **39,** 2417–2426.
23. Huang, Y. J., Cideciyan, A. V., Papastergiou, G. I., Banin, E., Semple-Rowland, S. L., Milam, A. H. & Jacobson, S. G. (1998) *Invest. Ophthalmol. Visual Sci.* **39,** 2405–2416.
24. Saari, J. C., Garwin, G. G., Van Hooser, J. P. & Palczewski, K. (1998) *Vision Res.* **38,** 1325–1333.
25. Yoshizawa, T. & Wald, G. (1963) *Nature (London)* **197,** 1279–1287.
26. Crouch, R. & Katz, S. (1980) *Vision Res.* **20,** 109–115.
27. Choo, D. W., Cheung, E. & Rando, R. R. (1998) *FEBS Lett.* **440,** 195–198.
28. Simon, A., Hellman, U., Wernstedt, C. & Eriksson, U. (1995) *J. Biol. Chem.* **270,** 1107–1112.
29. Foxman, S. G., Heckenlively, J. R., Bateman, J. B. & Wirtschafter, J. D. (1985) *Arch. Ophthalmol.* **103,** 1502–1506.
30. Fulton, A. B., Hansen, R. M. & Mayer, L. (1996) *Arch. Ophthalmol.* **114,** 698–703.
31. Simovich, M. J., Miller, B. E., Fulmer, C., McLeod, G. I., Kirkland, B. T., Davenport, C. M., Hanna, D. B., Nathans, J., Jacobson, S. G. & Pittler, S. J. (1999) *Invest. Ophthalmol. Visual Sci.* **40,** S470.
32. Cideciyan, A. V., Haeseleer, F., Fariss, R. N., Aleman, T. S., Jang, G-F., Verlinde, C. L. M. J., Marmor, M. F., Jacobson, S. G. & Palczewski, K. (2000) *Vis. Neurosci.*, in press.
33. Huang, Y., Cideciyan, A. V., Aleman, T., S., Banin, E., Huang, C. J., Syed, N. A., Petters, R. M., Wong, F., Milam, A. H. & Jacobson, S. G. (2000) *Exp. Eye Res.* **70,** 247–251.
34. Aguirre, G. D., Baldwin, V., Pearce-Kelling, S., Narfström, K., Ray, K. & Acland, G. M. (1998) *Mol. Vis.* **4,** 23.
35. Veske, A., Nilsson, S. E. G., Narfstrom, K. & Gal, A. (1999) *Genomics* **57,** 57–61.
36. Factorovich, E. G., Steinberg, R. H., Yasumura, D., Matthes, M. T. & LaVail, M. M. (1990) *Nature (London)* **347,** 83–86.
37. Berson, E. L., Rosner, B., Sandberg, M. A., Hayes, K. C., Nicholson, B. W., Weigel-DiFranco, C. & Willett, W. (1993) *Arch. Ophthalmol.* **111,** 761–772.
38. Bennett, J., Tanabe, T., Sun, D., Zeng, Y., Kjeldbye, H., Gouras, P. & Maguire, A. M. (1996) *Nat. Med.* **2,** 649–654.
39. Li, T. S., Sandberg, M. A., Pawlyk, B. S., Rosner, B., Hayes, K. C., Dryja, T. P. & Berson, E. L. (1998) *Proc. Natl. Acad. Sci. USA* **95,** 11933–11938.
40. Lewin, A. S., Drenser, K. A., Hauswirth, W. W., Nishikawa, S., Yasumura, D., Flannery, J. G. & LaVail, M. M. (1998) *Nat. Med.* **4,** 967–971.
41. Gouras, P., Carr, R. E. & Gunkel, R. D. (1971) *Invest. Ophthalmol.* **10,** 784–793.
42. Jacobson, S. G., Cideciyan, A. V., Regunath, G., Rodriguez, F. J., Vandenburgh, K., Sheffield, V. C. & Stone, E. M. (1995) *Nat. Genet.* **11,** 27–32.
43. Dowling, J. E. & Wald, G. (1958) *Proc. Natl. Acad. Sci. USA* **44,** 648–660.
44. Kelloff, G. J., Crowell, J. A., Boone, C. W., Steele, V. E., Lubet, R. A., Greenwald, P., Alberts, D. S., Covey, J. M., Doody, L. A., Knapp, G. G., *et al.* (1994) *J. Cell. Biochem. Suppl.* **20,** 55–62.
45. Milam, A. H., Li, Z.-Y. & Fariss, R. N. (1998) *Prog. Retin. Eye Res.* **17,** 175–205.
46. Hicks, D. & Sahel, J. (1999) *Invest. Ophthalmol. Visual Sci.* **40,** 3071–3074.
47. Perrault, I., Rozet, J. M., Gerber, S., Ghazi, I., Leowski, C., Ducroq, D., Souied, E., Dufier, J. L., Munnich, A. & Kaplan, J. (1999) *Mol. Genet. Metab.* **68,** 200–208.